atoms

MDPI

Article

High-Resolution Laboratory Measurements and Identification of Fe IX Lines near 171 Å

Peter Beiersdorfer [1,2,*], Jaan K. Lepson [1], Gregory V. Brown [2], Natalie Hell [2], Elmar Träbert [2,3], Michael Hahn [4] and Daniel W. Savin [4]

[1] Space Sciences Laboratory, University of California, Berkeley, CA 94720, USA
[2] Lawrence Livermore National Laboratory, Physics Department, Livermore, CA 94551, USA
[3] Fakultät für Physik und Astronomie, Ruhr-Universität Bochum, AIRUB, 44780 Bochum, Germany
[4] Columbia Astrophysics Laboratory, Columbia University, New York, NY 10027, USA
* Correspondence: beiersdorfer@berkeley.edu

Abstract: A multitude of weaker Fe IX lines have been predicted in the vicinity of the strong 171 Å line that dominates the spectra of many astrophysical and laboratory sources. Some of these weaker lines have only recently been identified in the laboratory, albeit some only tentatively. Here, we present measurements on the Livermore EBIT-I electron beam ion trap that span the region from 170.0 to 173.6 Å, which surrounds the 171 Å line. The measurements stepped through electron beam energy to determine the charge state of iron associated with each observed feature. Moreover, we have minimized the presence of oxygen in the trap, because oxygen lines obscured possible Fe IX lines in past measurements and prevented their identification. Our measurement confirms formerly tentative identifications and adds several new assignments.

Keywords: atomic spectra; line identification; extreme ultraviolet

check for updates

Citation: Beiersdorfer, P.; Lepson, J.K.; Brown, G.V.; Hell, N.; Träbert, E.; Hahn, M.; Savin, D.W. High-Resolution Laboratory Measurements and Identification of Fe IX Lines near 171 Å. *Atoms* **2022**, *10*, 148. https://doi.org/10.3390/atoms10040148

Academic Editors: Izumi Murakami, Daiji Kato, Hiroyuki A. Sakaue and Hajime Tanuma

Received: 24 September 2022
Accepted: 2 December 2022
Published: 8 December 2022

Publisher's Note: MDPI stays neutral with regard to jurisdictional claims in published maps and institutional affiliations.

Copyright: © 2022 by the authors. Licensee MDPI, Basel, Switzerland. This article is an open access article distributed under the terms and conditions of the Creative Commons Attribution (CC BY) license (https://creativecommons.org/licenses/by/4.0/).

1. Introduction

Emission from Fe IX have been observed in laboratory plasmas, for example, those produced in magnetic fusion devices [1–4], and in space plasmas, for example, in stellar coronae, including the Sun [5–10]. The strongest Fe IX line in the extreme ultraviolet wavelength band is situated at 171 Å and is well known. However, because of the complexity of the level structure of the 18-electron, argonlike Fe^{8+} ion, calculations predict a plethora of weak lines near the 171 Å line that have not been unequivocally observed and cataloged. This point is illustrated by the entries found for Fe IX transitions in the current version of the CHIANTI spectral database (V10.0.2), which lists 134 transitions in the wavelength interval between 170 and 172 Å, of which only the strong 171 Å line is deemed verified by observations [11]. Most of the remaining 133 transitions are predicted to be too weak to observe in low-density plasmas. Just a few are predicted to be strong enough to observe, and some progress was recently made in identifying Fe IX lines near 171 Å in experiments using an electron beam ion trap [12].

In the following, we build on the recent work at the EBIT-I electron beam ion trap at Livermore [12]. We present spectra in the narrow wavelength interval between 170.0 and 173.6 Å, in which we identify 11 Fe IX line features in addition to the strong 171 Å line. Our measurements confirm the identity of all but one of the lines previously identified as tentative Fe IX lines. In addition, we added five new lines to the list of Fe IX identifications. These include two lines that were previously predicted to blend with oxygen lines.

2. Experiment

The present measurements were carried out at EBIT-I, which was designed and built at the Lawrence Livermore National Laboratory as a spectroscopic facility [13,14] and is used, for example, for investigating spectra of astrophysical [15,16] and magnetic fusion

interest [17]. It has an electron density of typically $\leq 5 \times 10^{11}$ cm^{-3} [18,19], which is within the range of solar coronal electron densities [20].

The experimental conditions are similar to those described previously [12]. The ionization stage of iron is determined by the electron beam energy, as the ions are stripped of electrons up to the limit imposed by their ionization potential, including that of ions in metastable states. Lower charge states are also abundant, because we continuously inject iron in the form of iron pentacarbonyl ($Fe(CO)_5$). All of the observed lines are collisionally excited by electrons in the beam.

Our spectral observations were made with a high-resolution grazing-incidence grating spectrometer (HiGGS) designed for wavelength measurements above 100 Å [21]. The instrument was equipped with a flat-field grating with variable line spacing that focuses on a cryogenically cooled (−110 °C) charge-coupled device camera with 1340 × 1300 pixels measuring 20 µm × 20 µm each. The average line spacing was 2400 lines/mm and the angle of incidence was 87.5°.

Unlike the earlier experiments in which the energy of the electron beam was varied to only provide a rough discrimination of charge states, the present measurements were performed at densely spaced energy intervals. Small changes in the beam energy enabled us to trace the production thresholds of each ionization stage of iron, as described elsewhere [22–24].

Typical spectra are shown in Figure 1. Each spectrum was accumulated for 60 min and filtered for cosmic ray events. The effective resolving power of these measurements is 3000, and was not optimized in these measurements.

The wavelength scale was calibrated by reference to known spectral lines of oxygen that fall within the range observed by our instrument (cf. Figure 1a). The oxygen line emission was recorded while injecting carbon dioxide into the trap. In previous experiments [12], the oxygen lines shown in Figure 1a could also be seen when injecting $Fe(CO)_5$. However, in the present measurements, we adjusted the operating parameters of our machine until we optimized the iron signal over that of oxygen, and the oxygen lines were not visible when injecting $Fe(CO)_5$, as illustrated in Figure 1b–e.

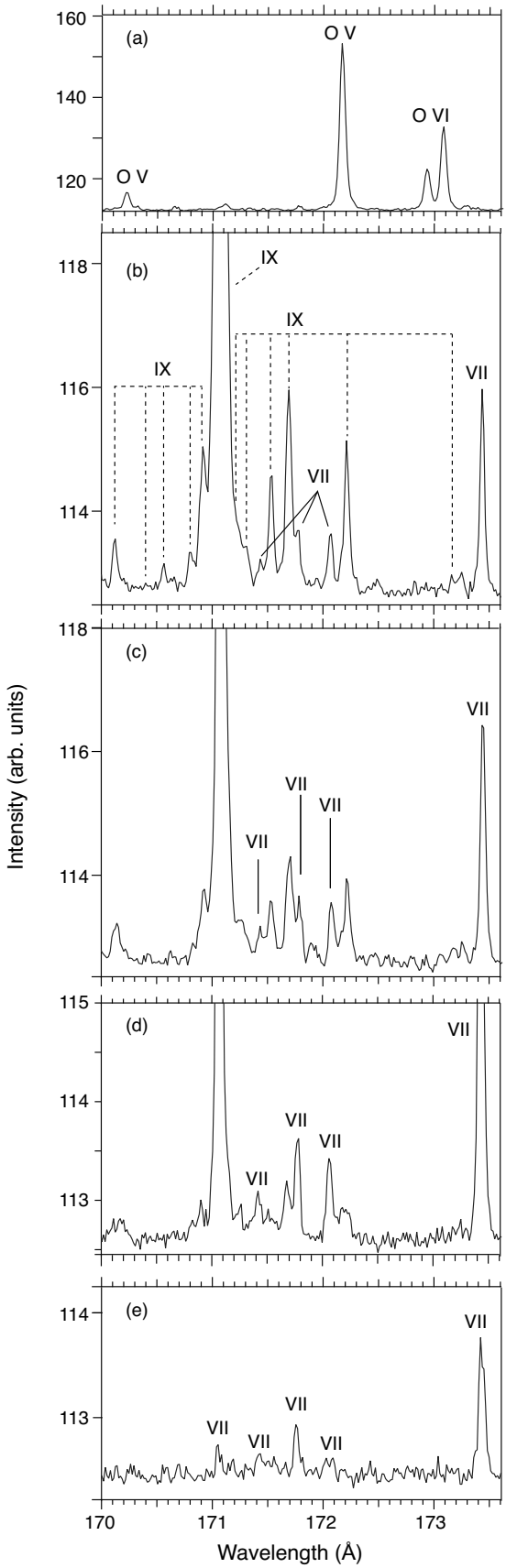

Figure 1. Spectra recorded on EBIT-I in the spectral range 170.0 to 173.6 Å: (**a**) Line emission from O V and O VI transitions; (**b**–**e**) line emission of Fe VII – Fe IX recorded at a nominal electron beam energy of (**b**) E_{beam} = 170 eV, (**c**) E_{beam} = 130 eV, (**d**) E_{beam} = 110 eV, and (**e**) E_{beam} = 90 eV.

3. Results

The iron spectra in Figure 1b–e illustrate the appearance of new lines as the beam energy threshold for the production of new charge states is crossed. At a nominal electron beam energy E_{beam} = 90 eV, only lines from Fe VII are visible in the spectrum (Fe VIII lines are not found in this wavelength interval, but they are monitored at wavelengths below 164 Å). As the beam energy is raised by 20 eV to E_{beam} = 110 eV, the strongest Fe IX line (at 171 Å) already dominates the spectrum. At E_{beam} = 130 eV the intensity of the Fe IX line increases even further and new lines, all attributable to weaker Fe IX lines, populate the spectrum. Finally, at E_{beam} = 170 eV, eleven Fe IX features, in addition to the strong Fe IX line at 171 Å can be identified in the spectrum. These features are labeled by capital letters *E* through *M* in Figure 2, in keeping with the labeling scheme used in [12], although labels *F* and *G* refer to more than one feature, as described below and given in Table 1.

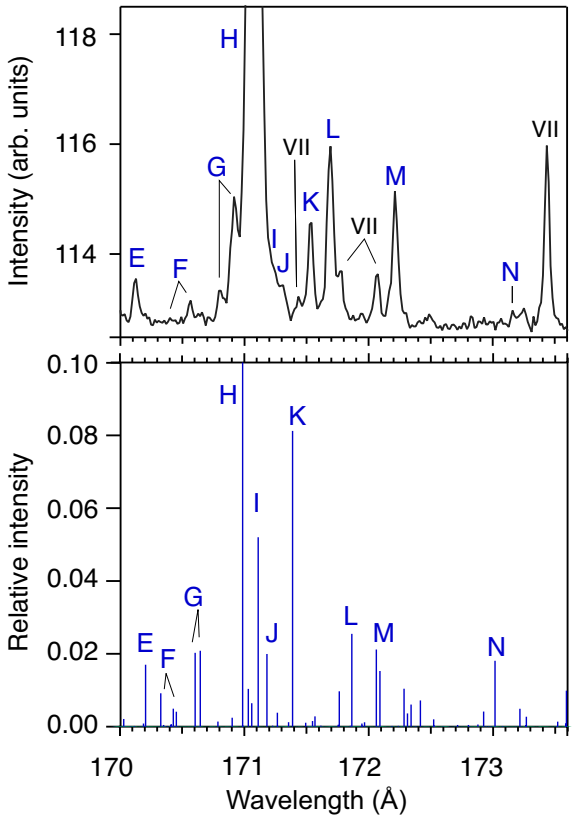

Figure 2. Comparison of measured spectral emission (**top**) with model predictions (**bottom**). The experimental data were produced at a nominal electron energy of E_{beam} = 170 eV. Predictions are based on MRMP and CRM calculations from Beiersdorfer et al. [25] performed at an electron density of 10^{10} cm^{-3} and an electron temperature of 54 eV. The calculations are normalized to the predicted intensity of line *H*, the Fe IX line at 171 Å.

Our new measurements confirm the Fe IX parentage of all but one of the lines that were tentatively identified earlier [12]. The lone exception is the line formerly labeled *L*, which is now confirmed to be an Fe VII feature. This feature sits on the short-wavelength side of the strong O V line (cf. Figure 1a) and it, therefore, was partially blended in previous measurements but it is now fully resolved.

We have identified five new Fe IX features. One of these, labeled *M* in Figure 2, was thought to be blended with the strong O V line in previous measurements. Because our iron spectra do not contain an oxygen line emission, line *M* is now fully resolved. Luckily, it is far enough away from the Fe VII line (mentioned above) that also blends with the O V so that the two features are fully resolved. Line *N* was also thought to be blended with a strong oxygen line, in this case the strong longer-wavelength O VI line shown Figure 1a.

In the absence of the O VI lines, we did not find a feature comparable in strength to line *M*. Instead, we note a weak feature on the long-wavelength side of the position of the O VI line that we labeled *N* in Figure 2. This feature may consist of two lines, both of which can be seen in Figure 1b,c, but at present is it not clear whether the second feature is indeed real. By contrast, we clearly see two features, labeled *G*, on the short-wavelength side of the strong 171 Å Fe IX line labeled *H*. The feature closest to line *H* was noted previously [12], but its parentage could not be determined. The other feature sits further to the short-wavelength side of *H* and was previously too uncertain to warrant mention. Finally, we observed a shoulder on the long-wavelength side of line *H* that sits between lines *H* and *J*. We labeled this feature *I* in Figure 2, as it appears to originate from Fe IX. Because the feature is highly blended, its identity, however, remains somewhat uncertain.

Table 1. Iron Fe IX lines observed in EBIT-I measurements. Wavelengths are in Å.

Key	Lower Level	Upper Level	λ [a]
E	$3s^2 3p_{1/2}^2 3p_{3/2}^3 3d_{5/2} (J=3)$	$3s^2 3p_{1/2}^2 3p_{3/2}^2 3d_{5/2}^2 (J=2)$	170.118
F-1	$3s^2 3p_{1/2}^2 3p_{3/2}^3 3d_{3/2}$ (J = 1)	$3s^2 3p_{1/2} 3p_{3/2}^3 3d_{5/2}^2 (J=2)$	170.41
F-2	$3s^2 3p_{1/2}^2 3p_{3/2}^3 3d_{3/2}$ (J = 1)	$3s^2 3p_{1/2}^2 3p_{3/2}^2 3d_{3/2} 3d_{5/2}$ (J = 1)	170.559 [b]
F-3	$3s^2 3p_{1/2} 3p_{3/2}^4 3d_{3/2}$ (J = 1)	$3s^2 3p_{3/2}^4 3d_{3/2} 3d_{5/2}$ (J = 1)	170.559 [b]
G-1	$3s^2 3p_{1/2} 3p_{3/2}^4 3d_{5/2} (J=2)$	$3s^2 3p_{3/2}^4 3d_{3/2} 3d_{5/2} (J=2)$	170.802
G-2	$3s^2 3p_{1/2} 3p_{3/2}^4 3d_{5/2} (J=2)$	$3s^2 3p_{1/2} 3p_{3/2}^3 3d_{3/2} 3d_{5/2} (J=1)$	170.915
H	$3s^2 3p_{1/2}^2 3p_{3/2}^4 (J=0)$	$3s^2 3p_{1/2}^2 3p_{3/2}^3 3d_{5/2}$ (J = 1)	171.073
I	$3s^2 3p_{1/2}^2 3p_{3/2}^3 3d_{5/2} (J=3)$	$3s^2 3p_{1/2}^2 3p_{3/2}^2 3d_{5/2}^2 (J=3)$	171.235
J	$3s^2 3p_{1/2}^2 3p_{3/2}^3 3d_{5/2} (J=2)$	$3s^2 3p_{1/2} 3p_{3/2}^3 3d_{3/2} 3d_{5/2} (J=1)$	171.312
K	$3s^2 3p_{1/2}^2 3p_{3/2}^3 3d_{5/2} (J=4)$	$3s^2 3p_{1/2}^2 3p_{3/2}^2 3d_{5/2}^2 (J=4)$	171.532
L	$3s^2 3p_{1/2}^2 3p_{3/2}^3 3d_{5/2} (J=2)$	$3s^2 3p_{1/2} 3p_{3/2}^3 3d_{5/2}^2 (J=2)$	171.690
M-1	$3s^2 3p_{1/2} 3p_{3/2}^4 3d_{3/2} (J=2)$	$3s^2 3p_{3/2}^4 3d_{3/2}^2 (J=2)$	172.215 [b]
M-2	$3s^2 3p_{1/2}^2 3p_{3/2}^3 3d_{5/2} (J=3)$	$3s^2 3p_{1/2}^2 3p_{3/2}^2 3d_{5/2}^2 (J=2)$	172.215 [b]
N	$3s^2 3p_{1/2} 3p_{3/2}^4 3d_{5/2} (J=3)$	$3s^2 3p_{1/2} 3p_{3/2}^3 3d_{5/2}^2 (J=2)$	173.16

[a] This work; [b] blend.

The labeling of the Fe IX features identified in our measurements follows the theoretical predictions in [12]. The predictions derived from a model based on the multi-reference Møller–Plesset (MRMP) calculations for the transition energies combined with collisional-radiative modeling (CRM) calculations for the line intensities that were developed in Beiersdorfer et al. [25]. The predictions of these calculations are shown in Figure 2 together with the experimental spectrum recorded at E_{beam} = 170 eV. We have simply labeled features from short to long wavelengths, employing the letters introduced in [12]. Because we have found four Fe IX features between lines *E* and *H*, we have (for now) assigned two of the features to *F* and two features to *G*.

The relative measured intensities roughly agree with the predicted intensities with two notable exceptions. The first concerns the two lines in feature *G*. The two lines are predicted to have equal intensities, but their relative intensities are measured to be 1:4. The second strong disagreement concerns line *K*. It is predicted to be stronger than any other Fe IX line in this wavelength region except line *H*. However, *K* is found to be weaker than features *L* and *M*. In other words, compared to features *L* and *M*, line *K* is only a third as strong as predicted. The predictions shown in Figure 2 were made for an electron density of 10^{10} cm^{-3} and an electron temperature of 68 eV, not for a mono-energetic electron beam. However, it was shown in [12] that the relative line ratios do not significantly change even for a mono-energetic electron beam or for different densities.

4. Discussion

Our present measurements have confirmed tentative identifications from previous measurements and have added new Fe IX features. Very importantly, the new measure-

ments agree reasonably well with spectral predictions. This gives us hope that further Fe IX line identifications are possible with the model in other wavelength intervals.

Author Contributions: Conceptualization, and data evaluation, P.B.; methodology, P.B., E.T.; experiment, P.B., N.H., G.V.B.; theory, P.B., J.K.L.; original draft preparation, P.B.; review and editing, P.B., D.W.S., J.K.L., E.T., N.H., G.V.B., M.H.; funding acquisition, P.B., D.W.S., M.H., G.V.B. All authors have read and agreed to the published version of the manuscript.

Funding: This work was supported by NASA H-TIDeS Grant No. 80NSSC20K0916 and was performed in part under the auspices of the U.S. Department of Energy by Lawrence Livermore National Laboratory under Contract DE-AC52-07NA27344.

Conflicts of Interest: The authors declare no conflict of interest.

References

1. Lepson, J.; Beiersdorfer, P.; Clementson, J.; Bitter, M.; Hill, K.W.; Kaita, R.; Skinner, C.H.; Roquemore, L.; Zimmer, G. High-resolution time-resolved extreme ultraviolet spectroscopy on NSTX. *Rev. Sci. Instrum.* **2012**, *83*, 10D520. [CrossRef]
2. Lepson, J.K.; Beiersdorfer, P.; Bitter, M.; Roquemore, A.L.; Kaita, R. Emission lines of iron in the 150–250 Å region on National Spherical Torus Experiment. *Phys. Scr.* **2013**, *T156*, 014075. [CrossRef]
3. Weller, M.E.; Beiersdorfer, P.; Soukhanovskii, V.A.; Magee, E.W.; Scotti, F. Three new extreme ultraviolet spectrometers on NSTX-U for impurity monitoring. *Rev. Sci. Instrum.* **2016**, *87*, 11E324. [CrossRef] [PubMed]
4. Lepson, J.K.; Beiersdorfer, P.; Bitter, M.; Roquemore, A.L.; Kaita, R. Unusual emission lines of carbon in the 170-190 Å region on NSTX. *AIP Conf. Ser.* **2017**, *1811*, 190008. [CrossRef]
5. Thomas, R.J.; Neupert, W.M. Extreme Ultraviolet Spectrum of a Solar Active Region from SERTS. *Astrophys. J.* **1994**, *91*, S461. [CrossRef]
6. Brosius, J.W.; Davila, J.M.; Thomas, R.J. Solar Active Region and Quiet-Sun Extreme-Ultraviolet Spectra from SERTS-95. *Astrophys. J.* **1998**, *119*, S255. [CrossRef]
7. Sirk, M.M.; Hurwitz, M.; Marchant, W. EUV Spectra of the Full Solar Disk: Analysis and Results of the Cosmic Hot Interstellar Plasma Spectrometer (CHIPS). *Sol. Phys.* **2010**, *264*, 287–309. [CrossRef]
8. Lepson, J.; Beiersdorfer, P.; Hurwitz, M.; Sirk, M.M.; Kato, T.; Yamamoto, N. Iron emission lines in solar and laboratory plasmas. *J. Phys. Conf. Ser.* **2008**, *130*, 012014. [CrossRef]
9. Raassen, A.J.J.; Mewe, R.; Audard, M.; Güdel, M.; Behar, E.; Kaastra, J.S.; van der Meer, R.L.J.; Foley, C.R.; Ness, J.U. High-resolution X-ray spectroscopy of Procyon by Chandra and XMM-Newton. *Astron. Astrophys.* **2002**, *389*, 228. [CrossRef]
10. Raassen, A.J.J.; Ness, J.U.; Mewe, R.; van der Meer, R.L.J.; Burwitz, V.; Kaastra, J.S. Chandra-LETGS X-ray observation of alpha Centauri: A nearby (G2V + K1V) binary system. *Astron. Astrophys.* **2003**, *400*, 671–678. [CrossRef]
11. Del Zanna, G.; Dere, K.P.; Young, P.R.; Landi, E. CHIANTI—An Atomic Database for Emission Lines. XVI. Version 10, Further Extensions. *Astrophys. J.* **2021**, *909*, 38. [CrossRef]
12. Beiersdorfer, P.; Träbert, E. High-resolution Laboratory Measurements of Coronal Lines near the Fe IX Line at 171 Å. *Astrophys. J.* **2018**, *854*, 114. [CrossRef]
13. Levine, M.A.; Marrs, R.E.; Bardsley, J.N.; Beiersdorfer, P.; Bennett, C.L.; Chen, M.H.; Cowan, T.; Dietrich, D.; Henderson, J.R.; Knapp, D.A.; et al. The use of an electron beam ion trap in the study of highly charged ions. *Nucl. Instrum. Methods* **1989**, *B43*, 431. [CrossRef]
14. Beiersdorfer, P. A "brief" history of spectroscopy on EBIT. *Can. J. Phys.* **2008**, *86*, 1. [CrossRef]
15. Beiersdorfer, P.; Brown, G.V.; Drake, J.J.; Gu, M.F.; Kahn, S.M.; Lepson, J.K.; Liedahl, D.A.; Mauche, C.W.; Savin, D.W.; Utter, S.B.; et al. Emission Line Spectra from Low-Density Laboratory Plasmas. *Rev. Mex. Astron. Astrofís.* **2000**, *9*, 123.
16. Beiersdorfer, P. Laboratory X-Ray Astrophysics. *Ann. Rev. Astron. Astrophys.* **2003**, *41*, 343. [CrossRef]
17. Beiersdorfer, P.; Clementson, J.; Safronova, U.I. Tungsten Data for Current and Future Uses in Fusion and Plasma Science. *Atoms* **2015**, *3*, 260–272. [CrossRef]
18. Chen, H.; Beiersdorfer, P.; Heeter, L.A.; Liedahl, D.A.; Naranjo-Rivera, K.L.; Träbert, E.; Gu, M.F.; Lepson, J.K. Experimental and Theoretical Evaluation of Density-sensitive N VI, Ar XIV, and Fe XXII Line Ratios. *Astrophys. J.* **2004**, *611*, 598. [CrossRef]
19. Arthanayaka, T.; Beiersdorfer, P.; Brown, G.V.; Gu, M.F.; Hahn, M.; Hell, N.; Lockard, T.; Savin, D.W. Laboratory Calibrations of Fe XII-XIV Line-intensity Ratios for Electron Density Diagnostics. *Astrophys. J.* **2020**, *890*, 77. [CrossRef]
20. Träbert, E.; Beiersdorfer, P.; Brown, G.V.; Hell, N.; Lepson, J.K.; Fairchild, A.J.; Hahn, M.; Savin, D.W. Laboratory search for Fe IX solar diagnostic lines at an electron beam ion trap. *Atoms* **2022**, *10*, 115. [CrossRef]
21. Beiersdorfer, P.; Magee, E.W.; Brown, G.V.; Hell, N.; Träbert, E.; Widmann, K. Extended-range grazing-incidence spectrometer for high-resolution extreme ultraviolet measurements on an electron beam ion trap. *Rev. Sci. Instrum.* **2014**, *85*, 11E422. [CrossRef] [PubMed]
22. Lepson, J.K.; Beiersdorfer, P.; Brown, G.V.; Kahn, S.M.; Liedahl, D.A.; Mauche, C.W.; Utter, S.B. Cataloguing Emission Line Spectra from Fe VII-Fe XXIV in the Extreme Ultraviolet. *Rev. Mex. Astron. Astrofís.* **2000**, *9*, 137.

23. Lepson, J.K.; Beiersdorfer, P.; Brown, G.V.; Liedahl, D.A.; Brickhouse, N.S.; Dupree, A.K.; Kaastra, J.S.; Mewe, R.; Kahn, S.M. Emission Lines of Fe VII-Fe X in the Extreme Ultraviolet Region, 60–140 Å. *Astrophys. J.* **2002**, *578*, 648. [CrossRef]
24. Lepson, J.K.; Beiersdorfer, P. Low-Energy Operation of the Lawrence Livermore Electron Beam Ion Traps: Atomic Spectroscopy of Si V, S VII and Ar IX. *Phys. Scr.* **2005**, *T120*, 62. [CrossRef]
25. Beiersdorfer, P.; Lepson, J.K.; Desai, P.; Díaz, F.; Ishikawa, Y. New Identifications of Fe IX, Fe X, Fe XI, Fe XII, and Fe XIII Lines in the Spectrum of Procyon Observed with the Chandra X-Ray Observatory. *Astrophys. J.* **2014**, *210*, 16. [CrossRef]